Original Research

The Influence of Natural Aging of the AW-2024 Aluminum Sheet on the Course of the Strain Hardening Curve

Stanisław Kut [1] iD **, Grzegorz Pasowicz [2],*** iD

[1] Department of Materials Forming and Processing, Faculty of Mechanical Engineering and Aeronautics, Rzeszow University of Technology, al. Powst. Warszawy 8, 35-959 Rzeszów, Poland

[2] Doctoral School of the Rzeszow University of Technology, al. Powst. Warszawy 12, 35-959 Rzeszów, Poland

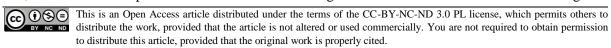* Correspondence: d546@stud.prz.edu.pl

Abstract

Aluminum sheet drawpieces pressings with the ability to harden precipitation can be shaped from the sheet after annealing or heat treatment. In the second variant during the analysis and design of the technological proces, the change in the material properties of the shaped sheet due to natural aging should be additionally taken into account. This article presents the results of research on the effect of the natural aging time after heat treatment of AW-2024 sheet material with a thickness of 1 mm on the course of the strain hardening curve. Strain hardening curves were determined on the basis of a uniaxial tensile test. The sheets were tested immediately after heat treatment and during natural aging, i.e. (20, 45, 90 and 120) minutes after heat treatment. The research showed a significant influence of natural aging in the tested range of times after heat treatment on the course of the deformation hardening curve of the sheet material. Based on experimentally determined in particular directions (0, 45 and 90 degrees to the rolling direction) the strain hardening curves, the values of material coefficients as a function of natural aging time were determined for four models of flow stress. Material coefficients in individual yield stress models were determined on the basis of approximation of strain hardening curves using the least squares method. On the basis of the analysis of approximation errors, the accuracy of the tested models of yield stress to describe the course of the hardening curve of the material of the tested sheet in the tested range of natural aging time was assessed.

Keywords: AW-2024 sheet, natural aging, strain hardening curves, strain hardening models, constitutive parameters

1. Introduction

Aluminum alloys, due to their properties (including high strength-to-weight ratio) and ease of production, are widely used in aviation and other areas of the transport industry (Polmear, 2006). They are the most widely used material in the production of aircraft. A practical example of this is AW-2024 (AlCu4Mg1) alloy. Its precipitation hardening ability is very often used to achieve the required mechanical properties (Davies, 2003; Kučera & Vojtěch, 2017). After solution treatment (heat treatment and aging), it shows relatively high strength and good fracture toughness (Miller et al., 2000; May et al., 2010; Sun et al., 2020). Aging after heat treatment may be natural or accelerated (artificial aging) (ASM International, 1991; Przybyłowicz, 2006). Natural aging gives better results in the form of increasing the strength of the drawpiece material than accelerated aging, but it lasts much longer, i.e., 4–5 days (Przybyłowicz, 2006). On the other hand, an increase in temperature causes a decrease in the accelerated aging time. Unfortunately, the material strength gets reduced after aging (ASM International, 1991; Przybyłowicz, 2006).

Aluminum sheet drawpieces pressings with the ability to harden precipitation can be shaped in two variants. In the first one, the sheets are shaped after softening annealing in the so-called "O" state, while the finished drawpieces undergo heat treatment and aging. On the other hand, in the second variant, the sheets are shaped after heat treatment. Forming the sheet after heat treatment is advantageous

because the drawpiece does not enter the furnace after forming, where it could deform during the heat treatment process by heating in the furnace followed by rapid cooling. Moreover, which is also very favorable, it is much easier to perform heat treatment of the sheets in the form of flat sheets than in the form of moldings formed therefrom with complex shapes.

However, after heat treatment during natural aging, there is an increase in strength and a decrease in deformability of the sheet material, which is unfavorable from the point of view of technological properties (Sobotka et al., 2018). The work (Fallah Tafti et al., 2018) presents the results of research on the variability of the microstructure as well as the strength and plastic properties of AW-2024 sheet 0.81 mm thick immediately after heat treatment and during natural aging for a specified time (0.5, 1.5, 4 and 24 hours) after heat treatment. The obtained results indicate that the greatest increase in strength properties occurred during natural aging up to 4 hours after heat treatment. For example, after 4 hours of aging, the yield point value increased by approx. 86% compared to the yield point immediately after heat treatment. However, in the tested time from 4 to 24 hours, the increase in the yield point was not so intense and amounted to only about 20% compared to the yield point after 4 hours of natural aging. Thus, the greatest increase in the strength properties, and the simultaneous decrease in deformability of the material occur in the first hours after heat treatment, i.e., the time when the drawpieces according to the second variant are formed, i.e., from sheet metal after heat treatment. Therefore, the parameters of the drawpieces shaping process (e.g., forming forces, susceptibility to plastic deformation) and the behavior of the material in this process (e.g., the amount of springback of the sheet) will significantly depend on the time after heat treatment in which a given technological operation will be carried out.

Due to the above, in engineering practice, forming sheet metal elements in the second variant, i.e., after heat treatment, requires taking into account the technological process called stamping. Changes in the properties of the sheet material (shaped in subsequent operations) occur as a result of natural aging. For this purpose, it is necessary to know the strength and plastic parameters as well as the material coefficients in the constitutive equations of the flow stress function depending on the natural aging time.

The aging process of the sheet material after heat treatment can be slowed down or delayed by lowering the temperature. The work (Sobotka et al., 2018). presents, inter alia, the results of research on the influence of the storage time in the freezer of sheet metal after heat treatment on its strength and plastic properties. The tests were carried out with the use of 2 mm thick AW-2024 sheet, which was stored in a freezer at -15 ˚C after heat treatment. Then, after (72, 120, 168 and 240) hours of storage in the freezer, uniaxial tensile tests were carried out in order to determine the strength and plastic properties. For the storage time in the freezer from 3 to 10 days, an almost 5% increase in the yield point was observed. At the same time, the elongation of Ag and A80 mm practically did not change. It is advantageous because storing the sheet in a freezer after heat treatment gives some possibilities related to the preparation and implementation of the entire technological and production process of sheet metal parts shaped in the second variant, i.e., after heat treatment. In industrial practice, the possibility of storing sheets after heat treatment in a freezer allows the process of forming a given batch of parts at a given production station at the same time after removal from the freezer, i.e., at the same stage of natural aging, which ensures repeatability of the technological properties of the charge sheet. For this reason, it is important when designing and analyzing the technological process of the drawpiece to determine at what stage of aging after heat treatment will be performed a specific operation of plastic forming of the part and to know the material parameters for this stage in the constitutive equations of yield stress.

As already mentioned, the analysis and design of the technological process of the sheet metal stamping after heat treatment requires, first of all, the knowledge of the material coefficients in the constitutive equations of flow stress as a function of natural aging time. Unfortunately, there are no studies in this field in the literature, which was the basis for the research presented in this article.

The aim of the research presented in this article was to determine the material coefficients for AW-2024 sheet with a thickness of 1 mm as a function of the natural aging time after heat treatment for four selected models of strain hardening. Knowing the values of these coefficients will make it possible to take into account the effect of changes in the properties of the sheet material resulting from natural aging after heat treatment in the analysis and design of technological processes and tooling in the stamping industry.

2. Test material and experimental procedure

The tested material was AW-2024 alclad sheet metal with a thickness of 1 mm. The chemical composition of the material of the tested sheet is presented in Table 1.

Table 1. Chemical composition of AW-2024 sheet material (European Committee for Standardization, 2007)

Si	Fe	Cu	Mn	Mg	Cr	Zn	Ti	Zr+Ti	Others		Aluminium min.
									Each	Total	
≤0.5	≤.5	3.8-4.9	0.3-0.9	1.2-1.8	≤0.1	≤0.25	≤0.15	≤0.2	0.05	0.15	Remainder

From this sheet as delivered, i.e., after softening annealing, samples were taken for uniaxial stretching in the directions (0, 45 and 90) degrees to the direction of sheet rolling. A total of 45 samples were prepared for the five aging time measurement points. The shape and dimensions of samples for testing in accordance with ISO 6892-1 are shown in Fig. 1.
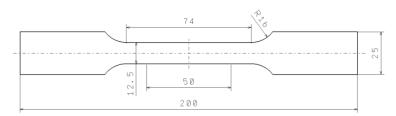

Fig. 1. Shape and dimensions of test specimens in mm

A solution heat treatment called heat treatment was carried out on the samples prepared in this way. The samples were successively heated in an oven to the temperature of 493 °C and kept at this temperature for 40 minutes (SAE International, 2015), and then subjected to rapid cooling in cold water. Then, uniaxial tensile tests were carried out successively immediately after heat treatment and during natural aging for 0, 20, 45, 90 and 120 minutes after heat treatment. The scope of aging time covered by the study was determined on the basis of an analysis of the range of manufactured drawpieces and engineering practice, taking into account the AMS2770 standard (SAE International, 2015). The time determined in this way was considered fully sufficient to complete the required technological operations of forming sheet metal parts. Such a time range was considered to be fully sufficient to carry out the required technological operations of shaping sheet metal parts. For each of the tested aging times after heat treatment, three samples were stretched in each direction. For this reason, in order to maintain the assumed time intervals between individual tests, solution heat treatment, and then uniaxial tensile tests were carried out in three rounds of 15 samples each. Static uniaxial tensile tests of individual samples were carried out successively on the Zwick / Roell Z030 testing machine with measurement of the elongation and change of the sample width using a multiextensometer (Fig. 2).

Fig. 2. An example of a sample during the uniaxial tensile test

3. Results and discussion

On the basis of the obtained results of experimental tests, the curves of strain hardening for particular directions (0˚, 45˚ and 90˚) and times after heat treatment were developed. Then, the values of material coefficients were determined for four selected constitutive models of flow stress with the determination of curve matching errors. The analysis of the influence of time after heat treatment on the value of the yield point and numerical values of the coefficients in selected constitutive equations was performed.

3.1. Influence of natural aging time on the yield point

The yield point is one of the basic strength parameters of the material, the numerical value of which significantly affects not only the forming forces and tool load, but also other parameters of the technological process, such as the amount of springback of the sheet. Therefore, it is important to know how this parameter changes with the aging time after heat treatment. The diagram (Fig. 3) shows the dependence of the yield strength of the tested sheet material as a function of the natural aging time after heat treatment. The numerical values for individual experimental points in the graphs present the arithmetic mean value obtained on the basis of three uniaxial stretching tests carried out in the same conditions. The obtained test results showed some differentiation of the strength and plastic properties of the tested sheet depending on the direction of sample collection (average normal anisotropy = 0.71 and its value practically did not depend on the aging time). The highest values of the yield point were in the 0˚ direction, slightly lower in the 90˚ direction, and the lowest in the 45˚ direction towards the rolling direction. In all directions, an almost linear increase in the yield strength was observed as a function of the natural aging time over the entire tested time range, i.e., (0–120) minutes. An approx. 40% increase in the yield point was observed. The position of the points on the graphs for the average value of individual parameters [$R_{p0.2-AV}$, B_{d-AV}, n_{1-AV}, K_{2-AV}, n_{2-AV}, σ_{0-AV}, A_{3-AV}, K_{3-AV}, n_{3-AV}, A_{4-AV}, B_{4-AV}, K_{4-AV}] described later in the article were calculated on the basis of the results for samples with different orientations in relation to the rolling direction according to the relationship:

$$X_{AV} = \frac{X_0 + 2X_{45} + X_{90}}{4} \tag{1}$$

where X is the parameter, and the subscripts denote the orientation of the specimen with respect to the rolling direction of the sheet.

As a result of the approximation of the experimental points, linear equations were obtained describing the increase in the yield point as a function of the natural aging time in particular directions. These equations for individual directions [$R_{p0.2-0}$ (t), $R_{p0.2-45}$ (t), $R_{p0.2-90}$ (t))] and for the average value [$Rp_{0.2-AV}$ (t)], were in the diagram (Fig. 3). In all cases, the correlation coefficient $R^2 > 0.99$.
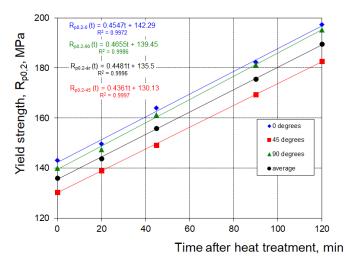

Fig. 3. Influence of aging time on the yield point

3.2. Influence of natural aging time on strain hardening curves

The hardening curves reflect the behavior of the material during plastic deformation. Their course describes the change in flow stress σ_p as a function of plastic strain ε_p. They are usually determined on the basis of uniaxial tensile, compression and torsion tests. Knowledge of the hardening curves is of great practical importance and is necessary for mathematical modeling of plastic forming processes.

The graph (Fig. 4) shows the experimentally determined curves of the material hardening of the tested sheet in the 0 ° direction for the tested times after heat treatment. On the other hand, in the graphs (Figs. 5 and 6), the curves of the strain hardening curve determined in the directions 45˚ (Fig. 5) and 90˚ (Fig. 6) for the same times after heat treatment. In all cases, a clear influence of the aging time on the course of the hardening curve was observed, with the aging time increasing the value of the flow stress σ_p proportionally over the entire range of plastic strain ε_p.
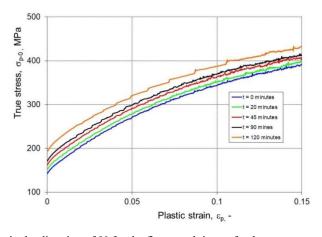

Fig. 4. Strain hardening curves in the direction of 0° for the five tested times after heat treatment
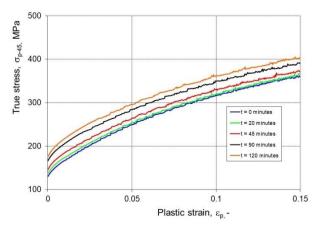

Fig. 5. Strain hardening curves in the direction of 45° for the five tested times after heat treatment
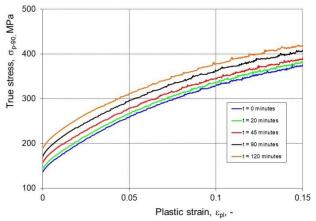

Fig. 6. Strain hardening curves in the direction of 90° for the five tested times after heat treatment

3.3. Selected functions of flow stress

For practical reasons, the curves of strain hardening are presented in the form of constitutive equations of the so-called function of flow stress. Such equations are used, inter alia, for the analysis and simulation of cold forming processes at relatively low strain rates, when their influence on the flow stress can be neglected. In this paper, four models of flow stress of various complexity levels were selected to describe the course of the material strain hardening of the tested sheet:

I. Hollomon (Hollomon, 1945)

$$\sigma_p(\varepsilon_p) = K_1 \varepsilon_p{}^{n_1} \tag{2}$$

II. Swift (Swift, 1952)

$$\sigma_p(\varepsilon_p) = K_2(\varepsilon_0 + \varepsilon_p)^{n_2} \tag{3}$$

III. Voce (Voce, 1948)

$$\sigma_p(\varepsilon_p) = A_3 + K_3\left(1 - \exp(-n_3\varepsilon_p)\right) \tag{4}$$

IV. Extended Voce (Stiebler et al., 1991)

$$\sigma_p(\varepsilon_p) = A_4 + B_4\varepsilon_p + K_4\left(1 - \exp(-n_4\varepsilon_p)\right) \tag{5}$$

where: σ_p – flow stress, ε_p – equivalent plastic strain, $K_1 \div K_4$, A_3, A_4, B_4, ε_0, $n_1 \div n_4$ – material constants determined experimentally.

The Hollomon model is the simplest and most often used in engineering practice, the strain hardening model, which provides a good description of the hardening curve in a wide range of deformation, which is why it is willingly used in modeling plastic forming processes, especially those with large deformations, such as forging, extrusion, punching, etc. The Swift model, like the Hollomon model, due to its versatility but also greater accuracy in the description of the initial course of the strain hardening curve, is very often used in numerical modeling of a wide range of plastic forming processes in the field of small and large deformations. Voce is also often used to describe the course of the strain hardening curve, which, like the Swift model, requires knowledge of three material constants. The most complex of the selected models is the extended Voce model with an additional linear component. Determination of the extended Voce model requires as many as four material constants. The extended Voce model is also referred to in the literature as the El-Magd model (Sener &Yurci, 2017).

3.4. Influence of constitutive equation on the error of matching curves of strain hardening

The material constants in equations (2)–(5) were determined for the individual strain hardening curves using the least squares method using the Logger Pro program. The error of fit B_d was calculated by relating the root mean square error RMSE to the mean feature level σ_p from the relationship:

$$B_d = \frac{RMSE}{(\sigma_p)_{av}} \cdot 100\% \tag{6}$$

The graphs (Figs. 7–10) summarize the calculated values of the error of matching the course of the strain hardening curves for each constitutive model, taking into account the directions of 0°, 45° and 90° depending on the natural aging time after heat treatment. The numerical values in the individual columns were calculated as the arithmetic average of the matching error on the basis of three uniaxial tensile tests carried out under the same conditions. The Hollomon model showed the largest matching error (slightly above 2%), which was practically independent of the aging time in the studied range (Fig. 7). In the case of using models with three material factors, the obtained error of matching was less than half that. In the case of these models, the matching error was influenced by both the sampling direction and the natural aging time after heat treatment. The Swift model showed the largest

error of matching in the 0˚ direction, and the smallest in the 90˚ direction (Fig. 8). On the other hand, the Voce model showed the greatest error of alignment in the 45˚ direction, and the smallest in the 0˚ direction (Fig. 9). Comparing the results for the Voce model with the results for the extended Voce model (Fig. 10), practically the same trend of the matching error distribution was observed, but the error of matching itself in the extended Voce model was the smallest among all the tested models. The effectiveness of individual models for describing the course of the hardening curves of the material of the tested sheet in terms of the tested aging times after heat treatment is best presented in the diagram (Fig. 11). The average error of matching for individual models was calculated from the dependence (1) on the basis of the error values calculated in the 0˚, 45˚ and 90˚ directions. As already mentioned, the largest average error of fit in the range (1.97–2.3%) was shown by the Hollomon model. In the case of the Swift model, the average matching error immediately after heat treatment was 0.95% and it decreased with the aging time reaching the value of 0.69% for the 120 minutes of aging time. for the Voce model, only slightly lower values of the average error of matching were obtained, but the average error of matching after heat treatment was 0.67% and (unlike the Swift model) it increased to 0.87% for the time of 120 minutes. As already mentioned, the same trend occurred in the case of the extended Voce equation, except that the average matching error was at the lowest level, ranging from 0.49% after heat treatment to 0.7% for an aging time of 120 minutes after heat treatment.
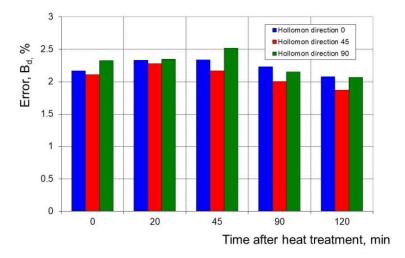

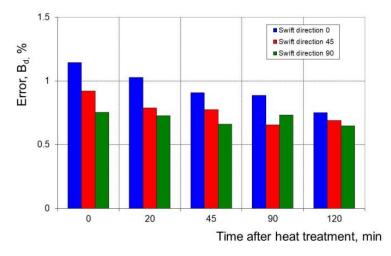**Fig. 7.** The matching Error of the curve by the Hollomon equation

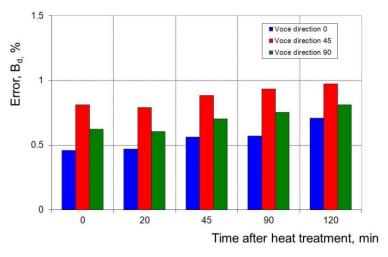**Fig. 8.** The matching Error of the curve by the Swift equation

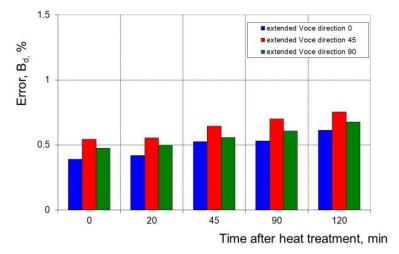**Fig. 9.** The matching Error of the curve by the Voce equation

Fig. 10. The matching Error of the curve by the extended Voce equation
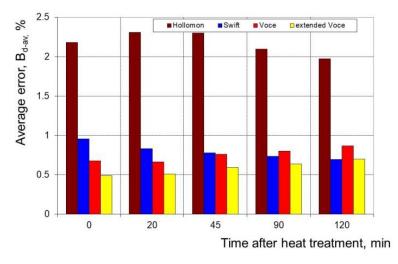

Fig. 11. Average matching error of curve for the tested models

3.5. Coefficients in constitutive equations as a function of aging time

In order to determine the dependence of the effect of the natural aging time after heat treatment on the value of the material coefficients in equations (2)–(5), graphs were prepared showing the dependence of individual coefficients as a function of the aging time after heat treatment. The points on the graphs for the 0˚, 45˚ and 90˚ directions (Fig. 12–23) present the arithmetic average value of

a given material factor, calculated on the basis of the approximation of the strain hardening curves for three tensile tests carried out under the same conditions. On the other hand, the location of the points for the average values of individual material parameters in these charts was calculated from the dependence (1).

In the case of the K_1 and K_2 coefficients in the Hollomon and Swift equations (Figs. 12 and 14), no specific trend was observed in aging after heat treatment in any of the directions. For this reason, the values of these coefficients were assumed to be constant in the range of the investigated heat treatment time, and their average value for each direction was calculated on the basis of five measurement points and presented in these graphs. On the other hand, a clear influence of the aging time was observed for the exponents of the strain hardening curves n_1 and n_2, respectively, in these equations (Figs. 13 and 15). In the case of these coefficients in all directions, a decrease in their value was observed with the aging time, and the trend was practically linear. As a result of the approximation of the experimental points with linear equations, the values of the coefficients in these equations were determined, which were presented in the graphs (Fig. 13 and 15) together with the values of the correlation coefficient R^2. In the case of the exponents n_1 and n_2, there was a high correlation, and the correlation coefficient for the average values of these coefficients was $R^2 > 0.99$. Among the respondents, only the coefficient ε_0 in the Swift equation did not show a typical linear trend. Therefore, in this case, the nonlinear equation presented in the graph was used for approximation (Fig. 16). In this case, the matching error for the average value $\varepsilon_{0\text{-}AV}$ calculated from the dependence (6) was 0.8%.
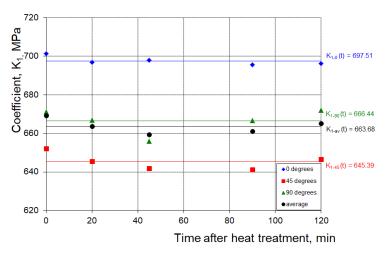

Fig. 12. Influence of aging time on the K_1 coefficient in the Hollomon equation
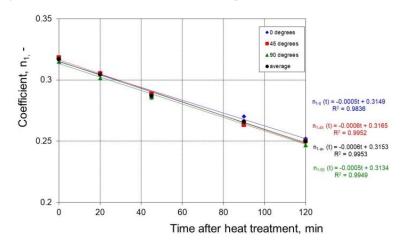

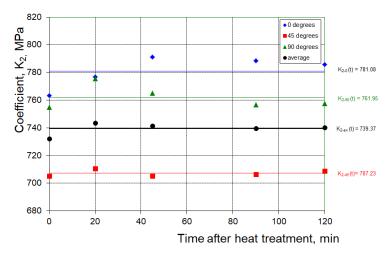**Fig. 13.** Influence of aging time on the n_1 coefficient in the Hollomon equation

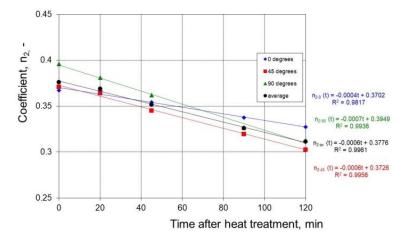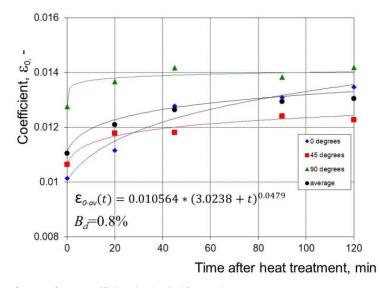**Fig. 14.** Influence of aging time on the K_2 coefficient in the Swift equation
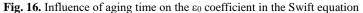

Fig. 15. Influence of aging time on the n_2 coefficient in the Swift equation

Fig. 16. Influence of aging time on the ε_0 coefficient in the Swift equation

In the case of the Voce model and the extended Voce model, practically all material coefficients showed an almost linear relationship in the tested aging time after heat treatment (Figs. 17–23). However, in the case of the A_3 and n_3 coefficients (Figs. 17 and 19), as well as A_4, B_4 and n_4 (Figs. 20, 21 and 23), an increase in their values was observed during aging after heat treatment. However, in the case of the remaining material coefficients K_3 (Fig. 18) and K_4 (Fig. 22), a decrease in their values was observed over time after heat treatment. As above, the calculated values of the coefficients in the line-

ar equations and the value of the correlation coefficient R^2 for each coefficient are presented in the form of equations in the graphs (Figs. 17–23).

The most important from the point of practical use of individual constitutive equations (e.g., in numerical modeling of the processes of forming the tested sheet metal after heat treatment) is the knowledge of the average value of material coefficients as a function of aging time after heat treatment. For this reason, the determined average values of the material coefficients for the tested strain hardening models as a function of the natural aging time after heat treatment are summarized in Table 2.
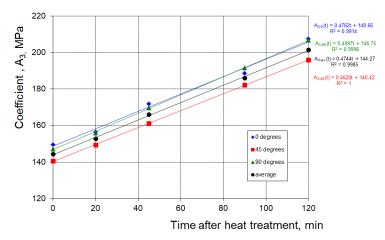

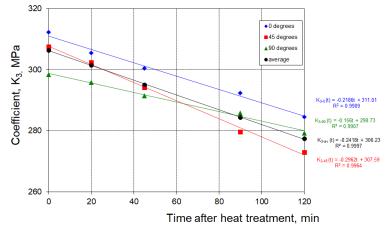**Fig. 17.** Influence of aging time on the A_3 coefficient in the Voce equation

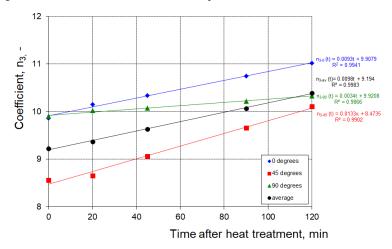**Fig. 18.** Influence of aging time on the K_3 coefficient in the Voce equation

Fig. 19. Influence of aging time on the n_3 coefficient in the Voce equation

Fig. 20. Influence of aging time on the A_4 coefficient in the extended Voce equation

Fig. 21. Influence of aging time on the B_4 coefficient in the extended Voce equation
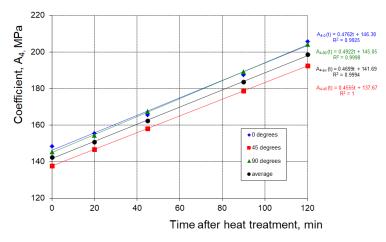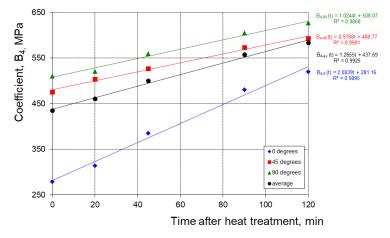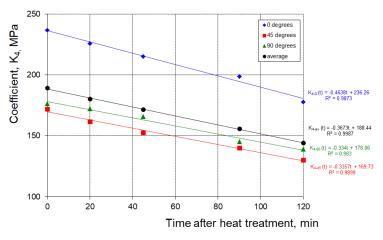

Fig. 22. Influence of aging time on the K_4 coefficient in the extended Voce equation
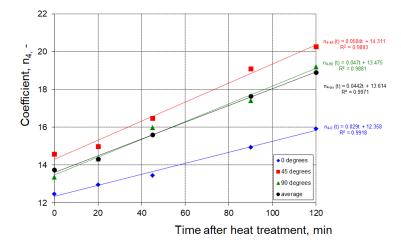
Fig. 23. Influence of aging time on the n_4 coefficient in the extended Voce equation

Table. 2. Experimentally determined material coefficients as a function of natural aging time in the range of 0–120 minutes after heat treatment for AW-2024 sheet with a thickness of 1 mm.

Strain hardening model		Coefficients as a function of aging time after heat treatment	Average value of the coefficient for the three directions	Correlation coefficient R^2
I	Hollomon	$K_1(t)$, MPa	663.68	-
		$n_1(t)$, -	$-0.0006t+0.3153$	0.9953
II	Swift	$K_2(t)$, MPA	739.37	-
		$\varepsilon_0(t)$, -	$0.0106*(3.0238+t)^{0.048}$	$B_d = 0.8\%$
		$n_2(t)$, -	$-0.0006t+0.3776$	0.9961
III	Voce	$A_3(t)$, MPa	$0.4744t+144.27$	0.9985
		$K_3(t)$, MPa	$-0.2418t+306.23$	0.9997
		$n_3(t)$, -	$0.0098t+9.194$	0.9983
IV	Extended Voce	$A_4(t)$, MPa	$0.4699t+141.69$	0.9994
		$B_4(t)$, MPa	$1.2655t+437.69$	0.9925
		$K_4(t)$, MPa	$-0.3673t+188.44$	0.9987
		$n_4(t)$, -	$0.0442t+13.614$	0.9971

4. Conclusions

In this article, on the basis of experimental tests for AW-2024 sheet with a thickness of 1 mm, material coefficients were determined in models of yielding stress as a function of natural aging time. Material coefficients were determined for four models: Hollomon, Swift, Voce and extended Voce. On the basis of the analysis of approximation errors, the usefulness of the tested models was assessed to describe the function of yielding stress of the tested sheet material after heat treatment and during natural aging in the examined time range. The range of aging time for which the tests were carried out and the values of material coefficients with excess were determined include the time during which individual operations of shaping the extrusions from heat-treated sheets are carried out. This ensures the possibility of analyzing and modeling individual stages of the molding process with the use of computer computational methods.

Based on the research, the following conclusions can be drawn:

1) In the scope of the tested aging time after heat treatment 0 ÷ 120 min, an approx. 40% increase in the yield point of the material of the tested sheet was found. Moreover, in the examined period of natural aging, the increase in the yield point was almost linear (correlation coefficient $R^2 > 0.99$).

2) Among the examined models of strain hardening, the extended Voce model ($B_{d\ av} \approx 0.58\%$) and the Voce model ($B_{d\ av.} \approx 0.75\%$) turned out to be the most accurate. The popular Swift

model was comparable ($B_{d\ av.} \approx 0.79\%$). It was observed that in the case of the Voce models, the error of matching increased with the aging time, while in the case of the Swift model it was the other way round, i.e., it decreased with aging time. In the case of the Hollomon model, the average error of matching was the highest and amounted to $B_{d\ av} \approx 2\%$.

3) In the studied range of aging, no clear trends were found in the course of the strain hardening factor K_1 in the Hollomon model and K_2 in the Swift model as a function of the aging time. For this reason, the average value for these coefficients from individual trials was adopted. The remaining coefficients in the tested strain hardening models showed a clear change in the aging time function, and their course was described with the use of linear equations, except for the ε_0 coefficient in the Swift model, the course of which was described by a power equation.

4) The dependence of the coefficients in the equations of flow stress on the time after heat treatment allows to easily take into account the change in technological properties of the material as a result of aging during the analysis and design of the molding processes in the second variant, i.e., after heat treatment.

References

ASM International. (1991). *ASM Handbook. Volume 4: Heat Treating ASM Handbook Committee*, 841-879. https://doi.org/10.1361/asmhba0001205

Davies, G. (2003). *Materials for automobile bodies*. Butterworth-Heinemann.

European Committee for Standardization. (2007). Aluminium and aluminium alloys - Chemical composition and form of wrought products - Part 3: Chemical composition and form of products (Standard No. EN 573-3).

Fallah Tafti, M. Sedighi, M., & Hashemi, R. (2018). Effects of natural ageing treatment on mechanical, microstructural and forming properties of Al 2024 aluminum alloy sheets. *Iranian Journal of Materials Science & Engineering, 15* (4), 1-10. https://doi.org/10.22068/ijmse.15.4.1

Hollomon, J. H. (1945) Tensile deformation. *Transactions of the Metallurgical Society of AIME*, *162*, 268-290.

Kučera, V., & Vojtěch D. (2017). Influence of the heat treatment on corrosion behavior and mechanical properties of the AA 7075 alloy. *Manufacturing Technology*, *17*(5), 747-752. https://doi.org/10.21062/ujep/x.2017/a/1213-2489/MT/17/5/747

May, A., Belouchrani, M.A., Taharboucht, S., & Boudras, A. (2010). Influence of heat treatment on the fatigue behaviour of two aluminium alloys 2024 and 2024 plated. *Procedia Engineering, 2(1)*, 1795-1804. https://doi.org/10.1016/j.proeng.2010.03.193

Miller, W.S., Zhuang, L., Bottema, J., Wittebrood, A.J., Smet, P.D., Haszler, A., & Vieregge, A. (2000). Recent development in aluminium alloys forthe automotive industry. *Materials Science and Engineering: A, 280 (1),* 37-49. https://doi.org/10.1016/S0921-5093(99)00653-X

Polmear I. (2006). *Light alloy: From traditional alloys to nanocrystals.* Butterworth-Heinemann.

Przybyłowicz K. (2006). *Metaloznawstwo*. Wydawnictwa Naukowo-Techniczne. In Polish.

SAE International. (2015). *Heat treatment of wrought aluminum alloy parts* (Standard No. AMS 2770R). Retrieved from https://www.sae.org/standards/content/ams2770r/

Sener B., & Yurci M. E. (2017). Comparison of quasi-static constitutive equations and modeling of flow curves for austenitic 304 and ferritic 430 stainless steels. *Acta Physica Polonica A*, *131* (3), 605-607. https://doi.org/10.12693/APhysPolA.131.605

Sobotka, J., Solfronk, P., Kolnerova, M., & Korecek D. (2018). Influence of technological parameters on ageing of aluminium alloy AW-2024. *Manufacturing Technology, 18*(6), 1023-1028. https://doi.org/10.21062/ujep/218.2018/a/1213-2489/MT/18/6/1023

Stiebler, K., Kunze, H., & El-Magd, E. (1991). Description of the of behaviour of a high strength austenitic steel under biaxial loading by a constitutive equation. *Nuclear Engineering and Design 127*(1), 85-93. https://doi.org/10.1016/0029-5493(91)90041-F

Sun, S., Fang, Y., Zhang, L., Li, Ch., & Hu, S. (2020). Effects of aging treatment and peripheral coarse grain on the exfoliation corrosion behaviour of 2024 aluminium alloy using SR-CT. *Journal of Materials Research and Technology*, *9*, 3219-3229. https://doi.org/10.1016/j.jmrt.2020.01.069

Swift, H.W. (1952). Plastic instability under plane stress. *Journal of the Mechanics and Physics of Solids 1* (1), 1-18. https://doi.org/10.1016/0022-5096(52)90002-1

Voce, E. (1948). The relationship between stress and strain for homogeneous deformations. *Journal of the Institute of Metals 74*, 537-562.

Wpływ Starzenia Naturalnego Blachy Aluminiowej AW-2024 na Przebieg Krzywej Umocnienia Odkształceniowego

Streszczenie

Wytłoczki z blach aluminiowych mających zdolność do utwardzania wydzieleniowego mogą być kształtowane z blachy po wyżarzaniu zmiękczającym lub po przesycaniu. W drugim przypadku podczas analizy i projektowania procesu technologicznego należy dodatkowo uwzględnić zmianę właściwości materiału kształtowanej blachy w wyniku starzenia naturalnego. W tym artykule przedstawiono wyniki badań wpływu czasu starzenia naturalnego po przesycaniu materiału blachy AW-2024 o grubości 1 mm na przebieg krzywej umocnienia odkształceniowego. Krzywe umocnienia zostały wyznaczone na podstawie próby jednoosiowego rozciągania. Badaniom poddano blachy bezpośrednio po przesycaniu oraz w trakcie starzenia naturalnego tj. (20, 45, 90 oraz 120) minut po przesycaniu. Badania wykazały, istotny wpływ starzenia naturalnego w badanym zakresie czasów po przesycaniu na przebieg krzywej umocnienia odkształceniowego materiału blachy. W oparciu o wyznaczone doświadczalnie na poszczególnych kierunkach (0, 45 oraz 90 stopni do kierunku walcowania) przebiegi krzywych umocnienia odkształceniowego wyznaczono wartości współczynników materiałowych w funkcji czasu starzenia naturalnego dla czterech modeli naprężenia uplastyczniającego. Współczynniki materiałowe w poszczególnych modelach naprężenia uplastyczniającego zostały wyznaczone na podstawie aproksymacji przebiegu krzywych umocnienia odkształceniowego metodą najmniejszych kwadratów. Na podstawie analizy błędów aproksymacji dokonano oceny dokładności badanych modeli naprężenia uplastyczniającego do opisu przebiegu krzywej umocnienia materiału badanej blachy w badanym zakresie czasu starzenia naturalnego.

Słowa kluczowe: blacha AW-2024, starzenie naturalne, krzywe umocnienia, modele umocnienia, stałe materiałowe